The Journal of Chemical Physics

Direct observation of mobility of thin polymer layers via asymmetric interdiffusion using neutron reflectivity measurements

Cite as: J. Chem. Phys. **151**, 244905 (2019); https://doi.org/10.1063/1.5132768
Submitted: 21 October 2019 . Accepted: 09 December 2019 . Published Online: 27 December 2019

Megumi Ooe, Kairi Miyata, Jun Yoshioka, Koji Fukao, Fumiya Nemoto, and Norifumi L. Yamada

The Journal of Chemical Physics ARTICLE scitation.org/journal/jcp

Direct observation of mobility of thin polymer layers via asymmetric interdiffusion using neutron reflectivity measurements

Cite as: J. Chem. Phys. 151, 244905 (2019); doi: 10.1063/1.5132768
Submitted: 21 October 2019 • Accepted: 9 December 2019 •
Published Online: 27 December 2019

Megumi Ooe,[1] Kairi Miyata,[1] Jun Yoshioka,[1] Koji Fukao,[1,a)] Fumiya Nemoto,[2,b)] and Norifumi L. Yamada[2]

AFFILIATIONS

[1] Department of Physics, Ritsumeikan University, Noji-Higashi 1-1-1, Kusatsu 525-8577 Japan
[2] Neutron Science Division, Institute for Materials Structure Science, High Energy Acceleration Research Organization, 203-1 Shirakata, Tokai, Naka 319-1106, Japan

[a)] **Author to whom correspondence should be addressed:** fukao.koji@gmail.com
[b)] **Present address:** Department of Materials Science and Engineering, National Defense Academy, 1-10-20 Hashirimizu, Yokosuka 239-8686, Japan.

ABSTRACT

In this study, we investigated the diffusion dynamics at the interface between deuterated poly(methyl methacrylate) (d-PMMA) and protonated poly(methyl methacrylate) (h-PMMA) in two-layered thin films of d- and h-PMMA layers via neutron reflectivity (NR) measurements during isothermal annealing above the glass transition temperature T_g. When T_g of d-PMMA was higher than that of h-PMMA, the d-PMMA layer thickness increased with increasing annealing time t_a and, simultaneously, the h-PMMA layer thickness decreased. However, the opposite t_a dependence of the layer thicknesses was observed, if the T_g of d-PMMA was decreased by the increase in the fraction of the low-molecular weight d-PMMA: With increasing t_a, the d-PMMA layer thickness decreased and the h-PMMA layer thickness increased when T_g of d-PMMA was lower than that of h-PMMA. This change in the t_a dependence of the layer thickness was related to the change in the mobility of the d-PMMA layer accompanied by the change in the T_g value of d-PMMA. With the decrease in the d-PMMA layer thickness from 49 nm to 13 nm, when the h-PMMA layer thickness was maintained, the t_a dependence of the layer thickness changed and the mobility of the d-PMMA layer dramatically increased. These results suggest that the mobility of thin polymer films can be determined by the observation of interfacial dynamics via NR measurements.

I. INTRODUCTION

Amorphous materials exhibit glass transition at which the thermal and mechanical properties change dramatically, although no structural change is typically accompanied by this transition.[1–3] The mechanism of the glass transition has been one of the most important problems in condensed-matter physics that needs to be solved.[4] Hence, glass transitions in confined geometries such as thin polymer films[5–9] and molecules in nanopores[10] have been intensively investigated in the past two decades. These studies have revealed a clear deviation of the glass transition temperature T_g from that of the bulk system via several experimental techniques.[7] Such a deviation from the bulk is thought to be strongly related to the physical mechanism of the glass transition. Recent studies have suggested that the glass transition and related dynamics in confined systems are governed by surface and interfacial effects,[11–14] as well as by the adsorption effect of polymer chains attached to the substrate.[15–17] Dynamical properties such as the glass transition of thin polymer films are controlled by the surface and interfacial effects and time-dependent properties of the adsorbed layers.[18]

Previous studies[8,9] investigated the glass transition and dynamics of the α-process in thin polymer films by dielectric relaxation spectroscopy (DRS). After the studies reported by Koh and Simon,[19,20] the T_g and α-process in stacked thin polymer films

such as polystyrene,[21] poly(methyl methacrylate) (PMMA),[22,23] and poly(2-chlorostyrene)[21,24] during annealing above T_g have been investigated by DRS and differential scanning calorimetry (DSC). This study revealed that the decreased T_g for the as-stacked thin films changes into the T_g of the bulk system; accordingly, the dynamics of the α-process changes from thin-film-like dynamics to the bulklike ones with the increase in the annealing time. These results suggest that interfacial interactions play a crucial role in determining the glass transition dynamics of thin polymer films.

Neutron reflectivity (NR) measurements constitute a powerful tool for determining the surface structure of thin films and the interface between two layers.[25,26] By NR, the thickness and density of thin layers and the roughness at the interface, which is the width of the interfacial region between two directly adjacent layers, can be examined.[27–38] In a study reported previously by our group, NR measurements were conducted in addition to DRS for multilayered thin films consisting of deuterated PMMA (d-PMMA) and protonated PMMA (h-PMMA) layers.[39] NR and DRS measurement results revealed that the time evolution of the structural change at the interface between the d- and h-PMMA layers is strongly correlated with that of the dynamics of the α-process during isothermal annealing above T_g. In this study, asymmetric interdiffusion at the interface between the two layers was also observed, i.e., the d-PMMA layer swells and the h-PMMA layer shrinks during annealing, when the T_g of d-PMMA was higher than that of h-PMMA. Such asymmetric interdiffusion is often observed for thin films composed of two layers with different mobilities.[32,37] Hence, the question of how the asymmetric interdiffusion can be correlated with the dynamics and T_g in thin polymer films needs to be answered.

In this study, NR measurements on different two-layered thin films of d- and h-PMMA layers were conducted to resolve the above-mentioned question. In Sec. III A, two-layered thin films of type I were used. Here, T_g of the d-PMMA layer was changed and T_g of the h-PMMA layer was maintained to investigate the correlation between the mobility difference between the two layers and the annealing-time dependence of the thickness of the two layers. In Sec. III B, two-layered thin films of type II were used. Here, the initial thickness of the d-PMMA layer was changed and that of the h-PMMA layer was maintained to investigate the thickness dependence of the interdiffusion at the interface between the two layers during annealing. Combining the results for these two types of two-layered thin films, we demonstrated the evaluation of the mobility of the d-PMMA layer from NR measurements. The obtained results suggest that there is a strong correlation between the interdiffusion at the interface and the dynamics of the thin polymer films.

II. EXPERIMENTS

A. Sample

Atactic h-PMMA and two d-PMMA with different molecular weights were used (Polymer Source, Inc.). The weight-average molecular weight M_w and the number-average molecular weight M_n of h-PMMA were 3.230×10^5 and 2.255×10^5, respectively, and the corresponding values for one type of d-PMMA (d-PMMA-1) were 2.63×10^5 and 2.29×10^5, and for the other type of d-PMMA (d-PMMA-2), they were 7.63×10^3 and 7.00×10^3. All eight hydrogen atoms of the h-PMMA monomer unit were replaced by deuterium to obtain the d-PMMA monomer. The scattering length densities (SLDs) of h-PMMA and d-PMMA monomers were 1.06×10^{10} cm^{-2} and 6.46×10^{10} cm^{-2}, respectively.[40] T_g values for bulk h-PMMA, d-PMMA-1, and d-PMMA-2 were 396.4 K, 403.1 K, and 384.0 K, respectively, which were measured by DSC during the heating process at 10 K/min.

TABLE I. Two-layered thin films of d-PMMA and h-PMMA layers of type I, for which the T_g value of the h-PMMA layer remains constant, while that of the d-PMMA layer changes between 403 K and 395 K upon blending of d-PMMA-1 and d-PMMA-2 with fractions from 1.0:0.0 to 0.6:0.4. Also shown in this table are the fraction between d-PMMA-1 and d-PMMA-2, initial thicknesses of h- and d-PMMA layers [$d_h(t_0)$ and $d_d(t_0)$, where t_0 is the initial time], and T_g of d-PMMA. The T_g value of h-PMMA is 396.4 K.

	d-PMMA-1/ d-PMMA-2	$d_h(t_0)$ (nm)	$d_d(t_0)$ (nm)	T_g (K) d-PMMA
PMMA-b1	1.0:0.0	25.3	35.2	403.1 K
PMMA-b2	0.9:0.1	26.5	27.7	402.0 K
PMMA-b3	0.8:0.2	30.1	32.8	400.9 K
PMMA-b4	0.6:0.4	32.2	34.9	395.3 K

B. Two-layered thin films

Two types of two-layered thin films of d-PMMA and h-PMMA were prepared. In the case of type I films, the thicknesses of d-PMMA and h-PMMA layers were maintained at ~30 nm (±5 nm). Only the T_g value of the d-PMMA layer was changed by blending d-PMMA-1 and d-PMMA-2 with various fractions (Table I). With the increase in the fraction of d-PMMA-2 from 0 to 0.4, the T_g value of d-PMMA-1 and d-PMMA-2 blend decreased from 403.1 K to 395.3 K, which was measured by DSC. On the other hand, T_g of h-PMMA remained constant at 396.4 K.

In the case of type II films, the thickness of the h-PMMA layer was ~25 nm, while that of the d-PMMA layer changed from 13 nm to 49 nm. In this case, only d-PMMA-1 was used for preparing d-PMMA layers (Table II).

These two-layered thin films were prepared on glass substrates by spin coating from a toluene solution. A thin d-PMMA layer was floated on the water surface and then transferred from the water

TABLE II. Two-layered thin films of d-PMMA and h-PMMA layers of type II, for which the thickness of the h-PMMA layer remains almost constant, while that of the d-PMMA layer changes from 13 nm to 49 nm. The d-PMMA layer consists of only d-PMMA-1.

	$d_h(t_0)$ of h-PMMA	$d_d(t_0)$ of d-PMMA
PMMA-t1	23.5 nm	13.0 nm
PMMA-t2	22.4 nm	24.8 nm
PMMA-t3	25.3 nm	35.2 nm
PMMA-t4	29.0 nm	48.7 nm

surface onto the glass substrate. Next, an h-PMMA layer was floated onto the water surface and transferred to the top of the d-PMMA layer on the substrate.

Notably, the thicknesses of the d- and h-PMMA layers given in Sec. II B correspond to those obtained by NR measurements at an initial time t_0 just after the temperature reaches the annealing temperature. Section II C provides the definition of t_0. The PMMA-b1 sample is the same as the PMMA-t3 sample. Different names are given to the same sample for comparison.

C. NR measurements

Time-resolved specular NR measurements were performed on the reflectometer: Soft Interface Analyzer [SOFIA, BL-16, Materials and Life Science Facility, Japan Proton Accelerator Research Complex (J-PARC), Tokai, Japan] with polychromatic wavelengths ranging from 0.25 nm to 1.76 nm (double frame mode).[41,42] The modulus of the neutron scattering vector for NR is $q = \frac{4\pi}{\lambda}\sin\theta$, where θ is the specular reflection angle and λ is the wavelength of neutrons. The θ value was set to 0.80° to obtain a q range of $0.1 < q < 0.8$ nm^{-1}. Two types of NR samples were mounted on a temperature-controllable sample cell. NR measurements were conducted during isothermal annealing at 409 K. The annealing time t_a is defined as the elapsed time from the time at which the sample temperature reaches 409 K. In our NR measurements, each data acquisition procedure starts at a time $t_a = t_0$ just after the time $t_a = 0$ at which the temperature reaches the annealing temperature. The t_0 value is ~0.05 h. The observed reflectivity profiles were analyzed using a program based on a recursion formula derived by Parratt,[43] together with dynamical correction according to the Névot-Croce extinction factor[44] to evaluate various parameters such as roughness and thickness that characterize the interface. In addition, a computer program, Motofit[45] in the Igor environment, was used for data fitting for comparison.

As fitting parameters for the two-layered thin films, two layer thicknesses of the d-PMMA, d_d, and h-PMMA, d_h, were evaluated, as well as two interfacial roughness values between the h- and d-PMMA layers, $r_{h/d}$, and between the air and h-PMMA layer, $r_{a/h}$ (Fig. 1). Two SLDs of the d-PMMA and h-PMMA layers, i.e., $\left(\frac{b}{V}\right)_d$ and $\left(\frac{b}{V}\right)_h$, were also used as fitting parameters. For both sample types, the roughness between the bottom layer and the substrate $r_{d/s}$ was considered and was maintained during data fitting.

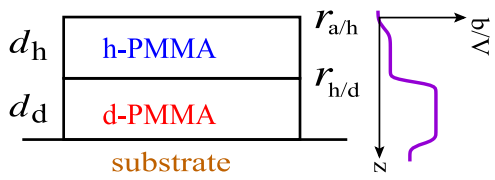

FIG. 1. (Left) Schematic of the two-layered thin films of h-PMMA and d-PMMA layers on the glass substrate, characterized by the thicknesses d_h and d_d, and roughnesses $r_{a/h}$ and $r_{h/d}$. (Right) Scattering length density as a function of the distance from the surface between the h-PMMA layer and air.

III. RESULTS AND DISCUSSION

A. NR of two-layered thin films of d-PMMA and h-PMMA of type I

1. NR and thickness of the d-PMMA and h-PMMA layers

Figure 2 shows the q dependence of the neutron reflectivity at various annealing times during isothermal annealing at 409 K for type I films (from PMMA-b1 to PMMA-b4). An appreciable change in the q dependence of NR was clearly observed. Solid curves were calculated using the two-layered model with the best fitting parameters obtained by data fitting. The sufficient agreement between the observed and calculated curves suggests the validity of the current two-layered model. Data fitting was performed under the condition that *the total scattering length, which was obtained after the integration of the SLD, ($\frac{b}{V}$), throughout the films, was conserved.* In addition, this condition is imposed for the data fitting of type II films also.

Figure S1 in the supplementary material shows the SLD profiles at various annealing times for type I film samples. With the increase in the annealing time, the SLD profile changed during isothermal annealing (Fig. S1). The SLD value for the d-PMMA layer decreased, while that for the h-PMMA layer increased with annealing. At the same time, the averaged position of the interface between the d-PMMA and h-PMMA layers shifted during annealing.

Figure 3 shows the annealing time dependence of the thicknesses of the h-PMMA and d-PMMA layers, d_h and d_d, relative to the initial thicknesses $d_h(t_0)$ and $d_d(t_0)$, respectively, for type I films. For PMMA-b1 (10:0), d_d increased with increasing t_a, while d_h decreased (Fig. 3). On the other hand, for PMMA-b4 (6:4), d_d decreased with t_a, while d_h increased with t_a. Here, the difference in the t_a dependence between PMMA-b1 and PMMA-b4 is thought to be attributed to the relationship between the glass transition temperature of d-PMMA, $T_{g,d}$, and that of h-PMMA, $T_{g,h}$: $T_{g,d}$ is higher than $T_{g,h}$ for PMMA-b1, while $T_{g,d}$ is lower than $T_{g,h}$ for PMMA-b4, as described in Sec. II B. Therefore, the discussion so far can be summarized by the use of the derivatives of d_d and d_h with respect to t_a as follows:

$$\frac{\partial d_d}{\partial t_a} > 0 \quad \text{and} \quad \frac{\partial d_h}{\partial t_a} < 0 \quad \text{for} \quad T_{g,d} > T_{g,h}, \tag{1}$$

$$\frac{\partial d_d}{\partial t_a} < 0 \quad \text{and} \quad \frac{\partial d_h}{\partial t_a} > 0 \quad \text{for} \quad T_{g,d} < T_{g,h}. \tag{2}$$

From these results, the annealing time dependence of the thicknesses of h-PMMA and d-PMMA layers is thought to be related to the difference in the glass transition temperature between the d-PMMA and h-PMMA, where the T_gs were measured by DSC for the bulk states.

2. Analysis of SLD profile by the total scattering length

In this section, the SLD profile is analyzed in further detail to introduce another important parameter for interdiffusion at the interface. Figure 4 shows an example of the dependence of SLD on the position from the surface in a direction normal to the layered thin film surface before and after 8 h of annealing at 409 K. The distance d_h corresponds to an averaged position of the interface between the h-PMMA and d-PMMA layers (Fig. 4). In this figure, d_h

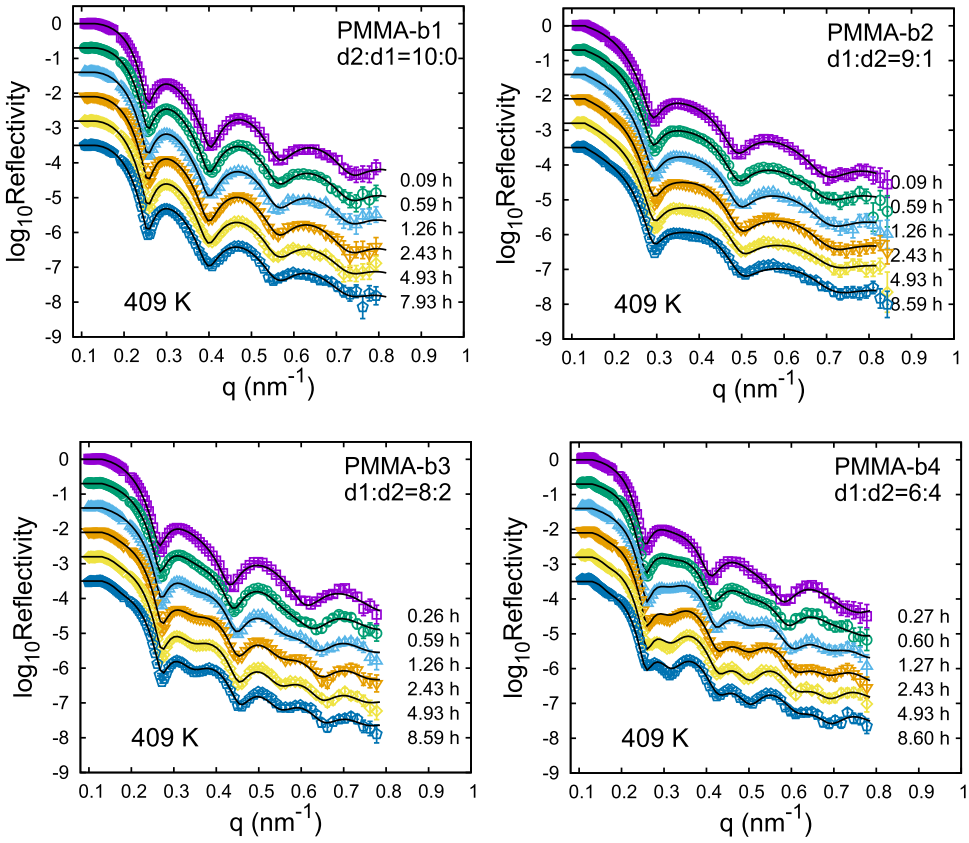

FIG. 2. Dependence of the neutron reflectivity on the modulus of the scattering vector q at various annealing times during annealing at 409 K for the two-layered thin films of d-PMMA and h-PMMA of type I.

is ~30 nm. The distance $d_d + d_h$ corresponds to the position of the interface between the d-PMMA and substrate. The $\left(\frac{b}{V}\right)_h$ and $\left(\frac{b}{V}\right)_d$ values correspond to the SLDs of the h-PMMA and d-PMMA layers, respectively. During isothermal annealing, interdiffusion occurs at the interface between h-PMMA and d-PMMA layers, leading to the exchange of d-PMMA and h-PMMA molecules through the interface. Hence, d_h, d_d, $\left(\frac{b}{V}\right)_h$, and $\left(\frac{b}{V}\right)_d$ values change with interdiffusion, in addition to the change in the roughness at the interfaces, i.e., the roughness $r_{h/d}$ at the interface between the d- and h-PMMA layers, which corresponds to the thickness of the crossover region between the d- and h-PMMA layers. In our analysis, the complementary error function erfc(z) is adopted to describe the shape of the SLD at the interface between the d-PMMA and h-PMMA layers.[32] In this case, the boundary between the d- and h-PMMA layers is defined as the center of the crossover region. Hence, the total scattering lengths per unit area of the h-PMMA and d-PMMA layers are defined by

$$\bar{b}_{\mathrm{tot,\,h}}(t_a) \equiv \left(\frac{b}{V}\right)_h \cdot d_h + \left(\left(\frac{b}{V}\right)_d - \left(\frac{b}{V}\right)_h\right)\frac{r_{h/d}}{\sqrt{2\pi}}, \tag{3}$$

$$\bar{b}_{\mathrm{tot,\,d}}(t_a) \equiv \left(\frac{b}{V}\right)_d \cdot d_d - \left(\left(\frac{b}{V}\right)_d - \left(\frac{b}{V}\right)_h\right)\frac{r_{h/d}}{\sqrt{2\pi}}, \tag{4}$$

respectively. Hereafter, the technical term "total scattering length" is used as the total scattering length *per unit area*.

During annealing, the total scattering length or the overall "mass" of the two-layered thin films should be conserved. This conservation law can be described by

$$\bar{b}_{\mathrm{tot,\,h}} + \bar{b}_{\mathrm{tot,\,d}} = \left(\frac{b}{V}\right)_h \cdot d_h + \left(\frac{b}{V}\right)_d \cdot d_d = \text{const.}, \tag{5}$$

where $\left(\frac{b}{V}\right)_h$, $\left(\frac{b}{V}\right)_d$, d_d, and d_h are values at any given value of the annealing time t_a. Here, the change in the total scattering length of the h-PMMA layer at t_a relative to the initial value at t_0 is defined as follows:

$$\Delta\bar{b}_{\mathrm{tot,\,h}}(t_a) = \bar{b}_{\mathrm{tot,\,h}}(t_a) - \bar{b}_{\mathrm{tot,\,h}}(t_0), \tag{6}$$

where $\bar{b}_{\mathrm{tot,\,h}}(t_a)$ and $\bar{b}_{\mathrm{tot,\,h}}(t_0)$ are the total scattering lengths of the h-PMMA layer at time t_a and t_0, respectively. Under the condition of Eq. (5), the change in the total scattering length of the d-PMMA layer at t_a relative to the initial value at t_0 is given by the relation

$$\Delta\bar{b}_{\mathrm{tot,\,d}}(t_a) = -\Delta\bar{b}_{\mathrm{tot,\,h}}(t_a). \tag{7}$$

In this current analysis, the law of conservation of mass or total scattering length is assumed; hence, the total volume of the two-layered films is not necessarily conserved. With the annealing time t_a, the layer thicknesses of d-PMMA d_d and h-PMMA d_h change without satisfying the relation $d_d + d_h$ = constant (Fig. 3). The present analysis is applicable even in the case when the total volume or averaged density is not constant.

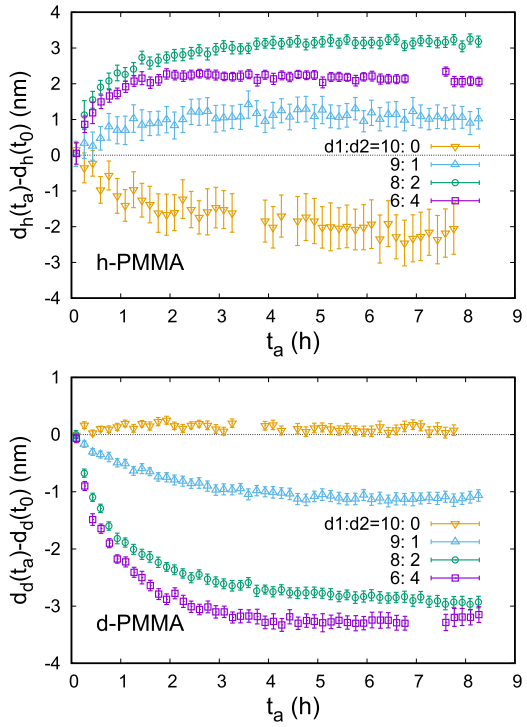

FIG. 3. Annealing time dependence of the thicknesses of h-PMMA (upper) and d-PMMA (lower) layers relative to the initial values at t_0 during isothermal annealing at 409 K for the two-layered thin films of d-PMMA and h-PMMA layers of type I. The fraction of d-PMMA-1 vs d-PMMA-2 changed from 10:0 to 6:4.

3. Total scattering length and the flow of d-PMMA and h-PMMA molecules

In the two-layered thin films, there is a chemical potential gradient with respect to each component of d-PMMA and h-PMMA and the chemical potential gradient changes with the annealing time during annealing. Hence, the flow of d-PMMA and h-PMMA molecules occurs so that the flux of d-PMMA, j_d (h-PMMA, j_h), is proportional to the chemical potential gradient of d-PMMA, $\Delta\mu_d$ (h-PMMA, $\Delta\mu_{dh}$),

$$j_i = \Lambda_{ii}\Delta\mu_i, \tag{8}$$

where $i = d$ for d-PMMA and $i = h$ for h-PMMA and Λ_{ii} is the Onsager coefficient.[46] The chemical potential gradient of d-PMMA (h-PMMA) is proportional to the concentration gradient of d-PMMA (h-PMMA),[47] indicating that there is a flow of d-PMMA molecules at the interface from the d-PMMA layer to the h-PMMA layer with the simultaneous flow of h-PMMA molecules at the interface from the h-PMMA layer to the d-PMMA layer during annealing. Two numbers are defined as follows: From t_0 to t_a, Δn_d is the number of d-PMMA molecules (monomers) that move through the interface of a unit area from the d-PMMA layer to the h-PMMA layer and Δn_h is the number of h-PMMA molecules (monomers) that move from the h-PMMA layer to the d-PMMA layer. Subsequently, the increase in the total scattering length of the h-PMMA layer can also be expressed by the increase in the net flow of the h-PMMA and d-PMMA monomers during annealing up to t_a as follows:

$$\Delta\bar{b}_{\mathrm{tot,h}}(t_a) = b_d\Delta n_d - b_h\Delta n_h, \tag{9}$$

where b_d (b_h) is the scattering length of one d-PMMA (h-PMMA) monomer. The b_d and b_h values are 98.2 fm and 14.9 fm, respectively.[40]

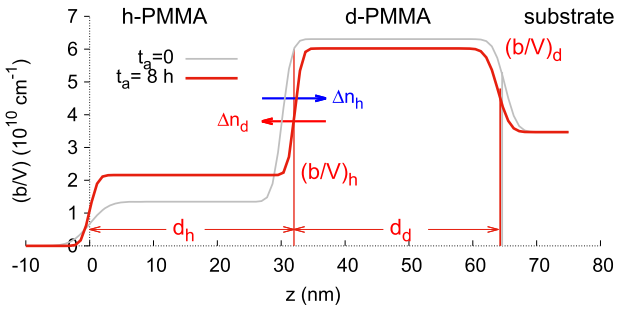

FIG. 4. Example of the profile of scattering length density (SLD) along the direction normal to the surface of the two-layered films of d-PMMA and h-PMMA on the glass substrate (PMMA-b4). Gray and red curves correspond to the profiles at the initial and final times (8 h) of annealing above T_g, respectively. The positions $z = 0$, d_h, and $d_h + d_d$ correspond to the surface of the two-layered thin films, the interface between h-PMMA and d-PMMA layers, and the interface between the d-PMMA layer and glass substrate, respectively.

4. Interdiffusion at the interface and scaling

From the observed dependence of the SLD profile on the annealing time t_a, the values $\Delta\bar{b}_{\mathrm{tot,h}}$ and $\Delta\bar{b}_{\mathrm{tot,d}}$ can be calculated by Eqs. (3), (4), (6), and (7) using the best-fitting parameters for $\left(\frac{b}{V}\right)_h$, $\left(\frac{b}{V}\right)_d$, d_h, d_d, and $r_{h/d}$. Figure 5 shows the t_a dependence of $\Delta\bar{b}_{\mathrm{tot,h}}$ observed for annealing at 409 K for type I films. The following results could be observed from Fig. 5(a):

1. $\Delta\bar{b}_{\mathrm{tot,h}}$ increases with t_a for the annealing of all four samples.
2. At a given value of t_a, the $\Delta\bar{b}_{\mathrm{tot,h}}$ value increases with the decrease in T_g of the d-PMMA layer.

With respect to result 1, the curves in Fig. 5(a) are given by the power-law equation as follows:

$$\bar{b}_{\mathrm{tot,h}}(t_a) = \bar{b}^0_{\mathrm{tot,h}} + \zeta t_a^{\alpha}, \tag{10}$$

where $\bar{b}^0_{\mathrm{tot,h}}$ is the value of $\bar{b}_{\mathrm{tot,h}}$ at $t_a = 0$, ζ is a positive constant, and α is the power-law exponent. In this case, simultaneous data fitting over all four samples revealed that $\alpha = 0.295 \pm 0.005$, although there might be some deviation from Eq. (10), i.e., some crossover to another power-law dependence for high fractions of low-molecular-weight components, for PMMA-b4. The exponent α is consistent with that observed for the time evolution of the width of the interface for PMMA[36] and with that of some quantities reported in our previous paper.[39] According to the Doi-Edwards theory on the dynamics of polymer chains, the time dependence of the root-mean-square displacement should follow a power-law with the exponent of 1/4 for the Rouse dynamics if the time region is shorter than the reptation time and larger than the Rouse time.[48] The observed value of the exponent α ~0.30 corresponds to the exponent 1/4, and hence,

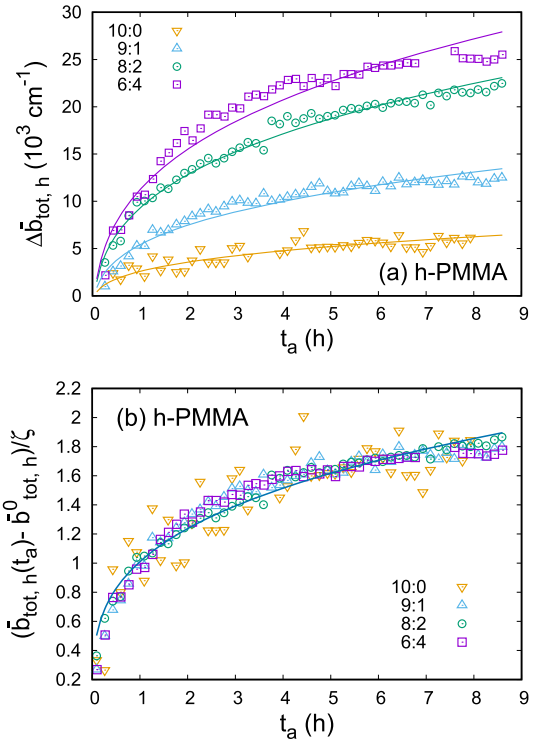

FIG. 5. (a) Annealing time dependence of the change in the total scattering length of the h-PMMA layer during annealing at 409 K for two-layered thin films of d- and h-PMMA of type I. T_g of the d-PMMA layer changes from 403 K to 395 K upon the blending of low- and high-molecular weight d-PMMA, while T_g of the h-PMMA layer remains constant at 396 K. The solid curves are calculated by Eq. (10). (b) The scaling plot of t_a dependence of $\bar{b}_{tot,h}(t_a)$ using Eq. (10) with the power-law exponent $\alpha = 0.295 \pm 0.005$.

the time evolution of $\bar{b}_{tot,h}$ may be related to that for the Rouse dynamics, as discussed in our previous paper.[39]

With respect to result 2, the dependence of $\Delta\bar{b}_{tot,h}$ on the T_g of the d-PMMA layer can be related to the following physical properties: the number Δn_d increases with the decrease in the T_g of d-PMMA, i.e., the enhanced mobility of the d-PMMA layer leads to the increase in the number of d-PMMA monomers moving from the d-PMMA layer to the h-PMMA layer due to the constant Δn_h value at a given value of t_a. Furthermore, Fig. 5(b) reveals that the data in Fig. 5(a) can be well reduced to a single master curve using Eq. (10), indicative of the presence of a common interdiffusion mechanism at the interface for type I films with various T_g values of the d-PMMA layer. Here, T_g of the d-PMMA layer is controlled by the addition of d-PMMA-2 (low molecular weight) into d-PMMA-1 (high molecular weight) with various fractions. In this case, the low-molecular-weight component of d-PMMA is expected to diffuse into the d-PMMA layer more easily than the high-molecular-weight component; hence, the interdiffusion at the interface may have a heterogeneous character. However, even in that case, the mobility of the d-PMMA layer can be well monitored by the total scattering length of the h-PMMA layer.

Here, it should be noted that there are several controlling parameters for the asymmetric interdiffusion at the interface such as T_g difference and molecular weight difference and so on. Because such parameters might be coupled with each other, more detailed and designed measurements will be required to clarify the mechanism of the asymmetric interdiffusion. This issue will be discussed in more detail in Sec. III A 5.

5. Swelling and mobility of thin polymer layers

Here, we attempt to interpret in more detail the dependence of $\Delta\bar{b}_{tot,h}$, Δn_d, and Δn_h on t_a and T_g, in addition to the dependence of the thicknesses d_d and d_h on t_a and T_g. According to the studies on interdiffusion for two-layered thin films of two polymeric systems with different mobilities during annealing,[49–52] fast-component molecules move into the slow-component layer via the interface between two layers; hence, the slow-component layer swells, i.e., the thickness of the slow-component layer increases with interdiffusion. For the PMMA-b4 (6:4) films, the molecular mobility of the d-PMMA layer is larger than that of the h-PMMA layer because of the lower T_g of the d-PMMA layer as compared with that of the h-PMMA layer. Hence, the d-PMMA molecules (fast-component) move into the h-PMMA layer (slow-component), and with the increase in the annealing time, the thickness of the h-PMMA layer increases, while that of the d-PMMA layer decreases (symbol □ in Fig. 3). As the number of the d-PMMA monomers in the h-PMMA layer increases with t_a because of interdiffusion, the total scattering length of the h-PMMA layer $\Delta\bar{b}_{tot,h}$ increases accordingly. For PMMA-b4 (6:4), $\Delta\bar{b}_{tot,h}$, Δn_d, and Δn_h values satisfy the following relationship:

$$\Delta\bar{b}_{tot,h} > 0 \quad \text{and} \quad \Delta n_d > \Delta n_h. \tag{11}$$

As shown in result 2 in Sec. III A 4, the total scattering length of the h-PMMA layer $\Delta\bar{b}_{tot,h}$ decreases with the increase in the T_g of the d-PMMA layer at a given t_a value, which is related to the decrease in the number Δn_d. For PMMA-b1 (10:0) films, the thickness of the d-PMMA layer increases with t_a, while that of the h-PMMA layer decreases with t_a, when T_g of the d-PMMA layer is higher than that of the h-PMMA layer. In this case, slow and fast components are d-PMMA and h-PMMA, respectively, within the Jabbari and Peppas model;[52] hence, Δn_h should be larger than Δn_d. Furthermore, the $\Delta\bar{b}_{tot,h}$ value is positive and slightly increases with t_a [Fig. 5(a)]. Hence, in the case of PMMA-b1, the following relationship should be valid:

$$\Delta\bar{b}_{tot,h} > 0 \quad \text{and} \quad \Delta n_h > \Delta n_d. \tag{12}$$

If the number Δn_h is not extremely large, i.e., Δn_h is less than $\frac{b_d}{b_h}\Delta n_d$, then the relationship in Eq. (12) can be satisfied, as described by Eq. (9). In the case of PMMA, the scattering length of the d-PMMA monomer is approximately seven times as large as that of the h-PMMA monomer, i.e., $b_d \approx 7b_h$. Even if the flow of h-PMMA monomers into the d-PMMA layer is stronger than that of the d-PMMA monomers into the h-PMMA layer, the change in the total scattering length $\Delta\bar{b}_{tot,h}$ can be positive and increases with t_a.

From NR measurements of type I films, the following results are obtained: The T_g difference between d-PMMA and h-PMMA, which was observed by DSC for the bulk states, is related to the

asymmetric interdiffusion of the polymer molecules at the interface between the h- and d-PMMA layers, which can be observed from the t_a dependence of the thicknesses d_h and d_d, and the change in the total scattering length $\Delta\bar{b}_{tot,h}$.

In this study, the d-PMMA layer was prepared by floating the spin-coated thin films, which were made from blending the two d-PMMAs with different molecular weights. DSC measurements showed that there is only one thermal anomaly in the temperature vs the total-heat-flow curve of the bulk of this blend, and hence, the initial state of the d-PMMA layer has a single T_g. The present measurements clearly showed that there is a relation between the annealing time dependence of the thickness of the h-PMMA and d-PMMA layers and the difference in "initial" T_g between the d-PMMA and h-PMMA. During the annealing, the low-molecular weight d-PMMA is expected to move faster than the high-molecular weight one. As a result, a heterogeneous structure may arise within the d-PMMA layer including the interfacial region. Furthermore, a T_g gradient also appears from the interface to the inside of the d-PMMA layer. In this case, the single T_g is not enough to describe the T_g of the d-PMMA layer and, hence, a distribution of T_g should be taken into account. To elucidate the distribution of T_g, we need more careful NR measurements clarifying the positional dependence of T_g and/or mobility. Nevertheless, the present measurements at least lead to the suggestion that the initial T_g difference between d-PMMA and h-PMMA can be one of the controlling parameters for asymmetric interdiffusion at the interface between the two layers during annealing.

Notably, the sign of the derivative of d_d (d_h) with respect to t_a changes between PMMA-b1 and PMMA-b2 (Fig. 3). However, the T_g of the bulk system given in Table I suggests that the above change in the sign of the derivative of d_d (d_h) should occur between PMMA-b3 and PMMA-b4. This apparent discrepancy may be solved if we adopt the T_g value of PMMA thin films with a thickness of 25–35 nm and not the T_g value of the bulk system.[6]

B. Two-layered thin films of d-PMMA and h-PMMA layers of type II

Section III B discussed the results obtained from NR measurements of type II films. In this type of two-layered thin films, the molecular weights and the geometry of the two thin layers are controlled to be the same within some uncertainty, except that only the thickness of the d-PMMA layer is changed from 13 nm (PMMA-t1) to 49 nm (PMMA-t4) to investigate the thickness dependence of the interfacial dynamics on the two-layered thin films.

1. NR and thickness of d-PMMA and h-PMMA layers

Figure 6 shows the dependence of NR on the modulus of scattering vector q for four type II two-layered thin films. In this figure,

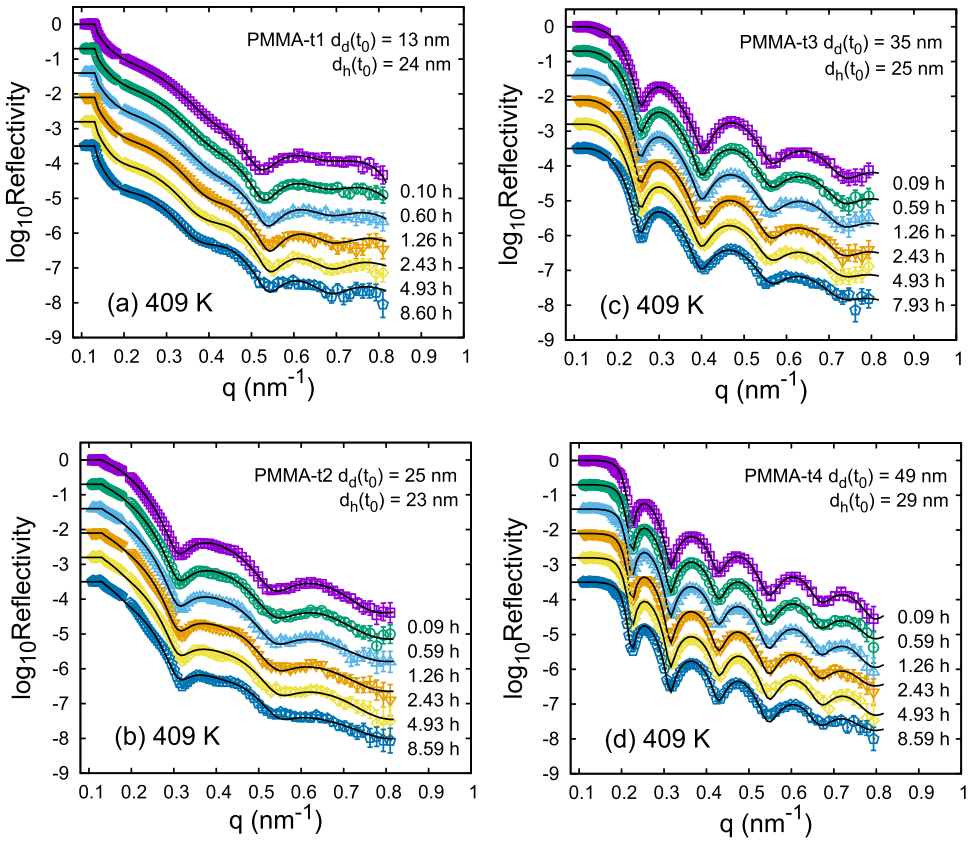

FIG. 6. Dependence of the neutron reflectivity on the modulus of the scattering vector at various annealing times during annealing at 409 K for the two-layered thin films of d- and h-PMMA layers of type II. Initial thickness of the d-PMMA layer changes from (a) 13 nm, (b) 25 nm, (c) 35 nm to (d) 49 nm.

the fringe period changes with the d-PMMA layer thickness and the q dependence of NR changes with the d-PMMA layer thickness. From the data fitting, the thickness of the two layers, roughness at two interfaces, and SLD of the d- and h-PMMA layers can be evaluated in the same manner as that done in Sec. III A. The solid curves in Fig. 6 are calculated using the best-fitting parameters. Figure S2 in the supplementary material shows the SLD profile of each sample. Here, the thicknesses of the two layers and the total scattering length of the h-PMMA layer as a function of the annealing time t_a and the initial thickness of the d-PMMA layer $d_d(t_0)$ are shown; these can be evaluated as the fitting parameters. Figure 7 shows the annealing time dependence of d_h and d_d during annealing at 409 K for type II films. For PMMA-t4 with $d_d(t_0)$ = 49 nm, d_h decreases with the increase in t_a and the t_a dependence of d_d is weaker than that for the other two-layered films with different $d_d(t_0)$ values (Fig. 7). For PMMA-t3 with $d_d(t_0)$ = 35 nm, d_h decreases with the increase in t_a in an almost similar manner as that observed for $d_d(t_0)$ = 49 nm, while d_d slightly increases with t_a. For PMMA-t2 with $d_d(t_0)$ = 25 nm, the derivative of d_d with respect to t_a becomes negative, i.e., d_d decreases and d_h slightly increases with the increase in t_a. Finally, for PMMA-t1 with $d_d(t_0)$ = 13 nm, d_d decreases and d_h increases with the increase in t_a and the changing amounts of d_h and d_d are considerably larger than those of PMMA-t2. Section III B 1 summarizes the following results:

$$\frac{\partial d_d}{\partial t_a} < 0 \quad \text{and} \quad \frac{\partial d_h}{\partial t_a} > 0 \quad \text{for} \quad d_d(t_0) = 13,\ 25\ \text{nm},$$
$$\frac{\partial d_d}{\partial t_a} > 0 \quad \text{and} \quad \frac{\partial d_h}{\partial t_a} < 0 \quad \text{for} \quad d_d(t_0) = 35,\ 49\ \text{nm}.$$

Hence, a strong dependence of d_d and d_h on the initial thickness of the d-PMMA layer could be observed.

2. Total scattering length, mobility, and T_g of h-PMMA and d-PMMA layers

Figure 8 shows the t_a dependence of the change in the total scattering length of the h-PMMA layer, $\Delta\bar{b}_{tot,h}(t_a)$, for type II films with various $d_d(t_0)$ values. With the increase in the annealing time, the total scattering length $\Delta\bar{b}_{tot,h}$ for all four samples increases, and at a given t_a value, $\Delta\bar{b}_{tot,h}$ values for $d_d(t_0)$ = 49 nm and 35 nm are almost equal to each other, and then, the total scattering length $\Delta\bar{b}_{tot,h}$ increases with the decrease in $d_d(t_0)$ from 35 nm to 13 nm during annealing at 409 K (Fig. 8). As $\Delta\bar{b}_{tot,h}$ is expressed by Eq. (9), the result in Fig. 8 suggests that the number of d-PMMA monomers moving through the interface from the d-PMMA layer to the h-PMMA layer, Δn_d, increases with the decrease in the d-PMMA layer thickness to less than 35 nm. Hence, the mobility of the d-PMMA layer increases with the decrease in the initial thickness of the d-PMMA layer. In other words, T_g of the d-PMMA layer may decrease with the decrease in $d_d(t_0)$.

Several studies have been reported on T_g of the thin films of PMMA.[6,53–56] The T_g value of thin PMMA films is well known to change with the interaction between the polymer and substrate.[57] For supported thin films, a dead layer with high T_g is expected to exist near the substrate.[5,9] In this case, the d-PMMA layer prepared by spin-coating is detached from the glass substrate to the water surface, which is then transferred from the water surface onto the glass substrate. Hence, a strong attractive interaction is not expected between the polymer and substrate. The present results of $\Delta\bar{b}_{tot,h}$ are consistent with those reported previously for the T_g value of thin PMMA films.

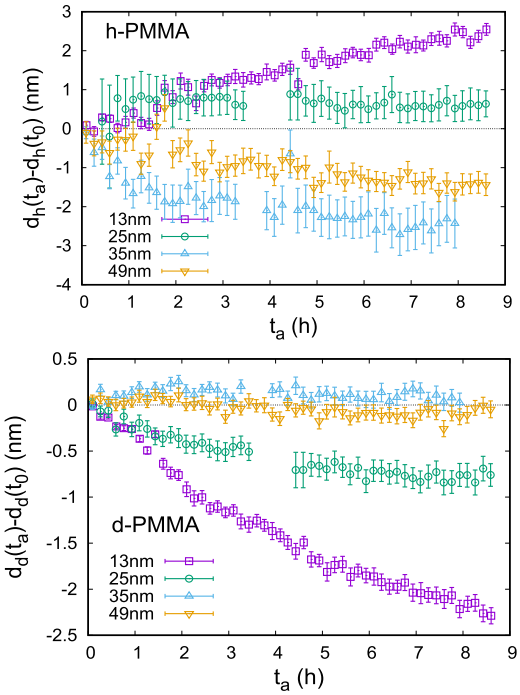

FIG. 7. Annealing time dependence of the thicknesses of h-PMMA (upper) and d-PMMA (lower) layers relative to those at the initial time t_0 during annealing at 409 K for the two-layered thin films of d- and h-PMMA of type II. The thickness d_d ranges from 13 nm to 49 nm, while the thickness d_h remains at ~25 nm (±3 nm).

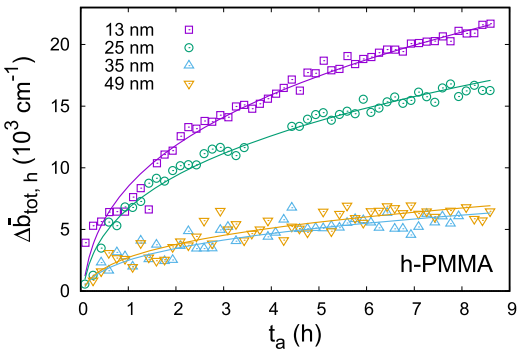

FIG. 8. Annealing-time dependence of the change in the total scattering length of the h-PMMA layer during annealing at 409 K for the two-layered thin films of d- and h-PMMA of type II. The initial thickness of the d-PMMA layer changes from 13 nm to 49 nm, while the initial thickness of the h-PMMA layer is constant at ~25 nm. The solid curves are calculated by Eq. (10) with α = 0.31 ± 0.03.

The solid curves in Fig. 8 are evaluated using Eq. (10) with the common exponent of $\alpha = 0.31 \pm 0.03$. This exponent is almost equal to that evaluated for type I films. Although the mobility of the d-PMMA layer changes with the film thickness, a common physical origin for the interdiffusion at the interface between the two layers should be present.

Here, the observed d_d, d_h, and $\Delta\bar{b}_{tot,h}$ as a function of t_a and $d_d(t_0)$ are discussed on the basis of the model introduced in Sec. III A. In type II films, the initial thickness of the h-PMMA layer $d_h(t_0)$ is ~25 nm and Δn_h should be the common function of t_a, regardless of $d_d(t_0)$. Hence, the $\Delta\bar{b}_{tot,h}$ value is expected to depend only on $\Delta n_d(t_a)$.

For $d_d(t_0) = 13$ nm, with increasing t_a, d_d decreases and d_h increases. At the same time, $\Delta\bar{b}_{tot,h}$ increases with t_a and it is larger than that of the other three type II samples at a given t_a value. Here, the observed $\Delta\bar{b}_{tot,h}$ value suggests that the mobility of the d-PMMA layer is highly enhanced compared with the bulk; it is larger than that of the h-PMMA layer, and $\Delta n_d > \Delta n_h$. In this case, d-PMMA and h-PMMA are the fast and slow components, respectively. Hence, the h-PMMA layer swells with an increase in t_a during annealing.

With the increase in $d_d(t_0)$ to 25 nm, Δn_d becomes smaller, because of the decrease in the total scattering length $\Delta\bar{b}_{tot,h}$ at a given t_a value. Even in this case, the relation $\Delta n_d > \Delta n_h$ is still valid because d_d decreases and d_h slightly increases with the increase in t_a. However, for $d_d(t_0) = 35$ nm, the derivative of the thickness d_d with respect to t_a becomes positive and that of the thickness d_h becomes negative. In this case, the d-PMMA layer swells with an increase in t_a. Hence, $\Delta n_d < \Delta n_h$, and the mobility of the d-PMMA layer becomes smaller than that of the h-PMMA layer. For $d_d(t_0) = 49$ nm, the $\Delta\bar{b}_{tot,h}$ value is almost equal to that for $d_d(t_0) = 35$ nm. This value is expected to be the same as that of the bulk system, and the mobility of the bulk is observed for $d_d(t_0) = 49$ nm and 35 nm. As for d_d, we observe the t_a dependence of d_d, which is similar to that observed for $d_d(t_0) = 35$ nm. However, the absolute thickness of the d-PMMA layer is larger than that for other samples; hence, the relative change in d_d apparently has statistical errors.

From the results observed in Sec. III B, the mobility of the d-PMMA thin layer, relative to that of the h-PMMA layer, can be well monitored by the change in the total scattering length of the h-PMMA layer $\Delta\bar{b}_{tot,h}$ as a function of t_a, which is evaluated from NR measurements. If the mobility of the other layer, i.e., the h-PMMA layer, is known, the absolute value of the mobility of the thin d-PMMA layer can be determined through the observation of the interdiffusion at the interface. Therefore, NR measurements can be a useful tool for the determination of the mobility of ultrathin polymer films, although the NR instrument is extremely expensive.

In this paper, we have successfully determined the mobility of the thin polymer layer, relative to that of the other thin polymer layer, by NR measurements during annealing at a given temperature. Further NR measurements during heating and cooling processes at a constant rate will give us a temperature dependence of the layer thicknesses of d-PMMA and h-PMMA from which a "thermodynamic" T_g can be determined. Combining the "dynamical" T_g value evaluated from the present mobility measurements, we can compare the two different T_gs and, hence, we will be able to investigate the possibility of a decoupling between the two T_gs and the validity of the so-called Frenkel-Kobeko-Reiner hypothesis.[58,59]

IV. CONCLUDING REMARKS

In this study, we investigated by NR measurements the relationship between the interdiffusion at the interface and the mobility difference during annealing above T_g for two-layered thin films of d-PMMA and h-PMMA layers on a glass substrate. The obtained results can be summarized as follows:

1. With the decrease in the T_g of the d-PMMA layer via the increase in the fraction of the low-molecular-weight d-PMMA, the number of d-PMMA monomers moving from the d-PMMA layer to the h-PMMA layer increases at a given annealing time t_a.
2. With the decrease in the thickness of the d-PMMA layer at a given t_a value, the number of d-PMMA monomers moving from the d-PMMA layer to the h-PMMA layer increases, suggesting that the mobility of the d-PMMA layer increases, and hence T_g decreases, with a decrease in the thickness of the d-PMMA layer.
3. The above results suggest that the NR measurements can be a useful tool for determining the mobility of thin polymer films.

In this study, there is a strong correlation between the asymmetric interdiffusion at the interface and the dynamics of thin polymer films. By using this correlation, the mobility of the thin polymer layer within multilayered thin films can be determined.

SUPPLEMENTARY MATERIAL

See the supplementary material for the scattering length density profile for the two-layered thin films of types I and II.

ACKNOWLEDGMENTS

K.F. would like to express his cordial thanks to Professor Keiji Tanaka of Kyushu University for his valuable comments on this study. This work was in part supported by the Grant-in-Aid for Scientific Research (B) (Grant Nos. 19H01865 and 16H04036) and Exploratory Research (Grant No. 18K18740) from the Japan Society for the Promotion of Science. Neutron reflectivity measurements were performed on BL-16 at the Materials and Life Science Facility, J-PARC, Japan, under the Program Nos. 2017B0034, 2018A0095, 2018B0154, and 2019A0142.

REFERENCES

[1] M. D. Ediger, C. A. Angell, and S. R. Nagel, J. Phys. Chem. **100**, 13200 (1996).
[2] K. L. Ngai, in *Physical Properties of Polymers*, edited by J. Mark (Cambridge University Press, 2004), pp. 72–152.
[3] C. B. Roth and R. R. Baglay, in *Polymer Glasses*, edited by C. B. Roth (CRC Press, 2016), pp. 3–22.
[4] P. W. Anderson, Science **267**, 1615 (1995).
[5] J. L. Keddie, R. A. L. Jones, and R. A. Cory, Europhys. Lett. **27**, 59 (1994).
[6] J. L. Keddie, R. A. L. Jones, and R. A. Cory, Faraday Discuss. **98**, 219 (1994).
[7] J. A. Forrest and R. A. Jones, in *Polymer Surfaces, Interfaces and Thin Films*, Advances in Polymer Science, edited by A. Karim and S. Kumar (World Scientific Publishing, 2000), pp. 251–294.
[8] K. Fukao and Y. Miyamoto, Europhys. Lett. **46**, 649 (1999).

[9]K. Fukao and Y. Miyamoto, Phys. Rev. E **61**, 1743 (2000).
[10]M. Alcoutlabi and G. B. McKenna, J. Phys.: Condens. Matter **17**, R461 (2005).
[11]M. D. Ediger and J. A. Forrest, Macromolecules **47**, 471 (2014).
[12]H. Kim, Y. Cang, E. Kang, B. Graczykowski, M. Secchi, M. Montagna, R. D. Priestley, E. M. Furst, and G. Fytas, Nat. Commun. **9**, 2918 (2018).
[13]E. Kang, H. Kim, L. A. G. Gray, D. Christie, U. Jonas, B. Graczykowski, E. M. Furst, R. D. Priestley, and G. Fytas, Macromolecules **51**, 8522 (2018).
[14]E. Kang, B. Graczykowski, U. Jonas, D. Christie, L. A. G. Gray, D. Cangialosi, R. D. Priestley, and G. Fytas, Macromolecules **52**, 5399 (2019).
[15]S. Napolitano, S. Capponi, and B. Vanroy, Eur. Phys. J. E **36**, 61 (2013).
[16]S. Napolitano, *Non-Equilibrium Phenomena in Confined Soft Matter*, Soft and Biological Matter (Springer International Publishing, Heidelberg, 2015), ISBN: 978-3-319-21948-6.
[17]S. Napolitano, E. Glynos, and N. B. Tito, Rep. Prog. Phys. **80**, 036602 (2017).
[18]M. J. Burroughs, S. Napolitano, D. Cangialosi, and R. D. Priestley, Macromolecules **49**, 4647 (2016).
[19]Y. P. Koh, G. B. McKenna, and S. L. Simon, J. Polym. Sci., Part B: Polym. Phys. **44**, 3518 (2006).
[20]Y. P. Koh and S. L. Simon, J. Polym. Sci., Part B: Polym. Phys. **46**, 2741 (2008).
[21]K. Fukao, T. Terasawa, Y. Oda, K. Nakamura, and D. Tahara, Phys. Rev. E **84**, 041808 (2011).
[22]T. Hayashi and K. Fukao, Phys. Rev. E **89**, 022602 (2014).
[23]K. Fukao, H. Takaki, and T. Hayashi, in *Dynamics in Geometrical Confinement*, Advances in Dielectrics, edited by F. Kremer (Springer International Publishing, 2014), pp. 179–212.
[24]K. Fukao, Y. Oda, K. Nakamura, and D. Tahara, Eur. Phys. J.: Spec. Top. **189**, 165 (2010).
[25]T. Russell, Mater. Sci. Rep. **5**, 171 (1990).
[26]N. Torikai, N. L. Yamada, A. Noro, M. Harada, D. Kawaguchi, A. Takano, and Y. Matsushita, Polym. J. **39**, 1238 (2007).
[27]P. F. Green, C. J. Palmstrom, J. W. Mayer, and E. J. Kramer, Macromolecules **18**, 501 (1985).
[28]E. A. Jordan, R. C. Ball, A. M. Donald, L. J. Fetters, R. A. L. Jones, and J. Klein, Macromolecules **21**, 235 (1988).
[29]S. F. Tead and E. J. Kramer, Macromolecules **21**, 1513 (1988).
[30]J. Von Seggern, S. Klotz, and H. J. Cantow, Macromolecules **22**, 3328 (1989).
[31]S. J. Whitlow and R. P. Wool, Macromolecules **22**, 2648 (1989).
[32]G. Reiter and U. Steiner, J. Phys. II **1**, 659 (1991).
[33]S. J. Whitlow and R. P. Wool, Macromolecules **24**, 5926 (1991).
[34]B. B. Sauer and D. J. Walsh, Macromolecules **24**, 5948 (1991).
[35]A. Karim, G. P. Felcher, and T. P. Russell, Macromolecules **27**, 6973 (1994).
[36]K. Kunz and M. Stamm, Macromolecules **29**, 2548 (1996).
[37]D. Kawaguchi, A. Nelson, Y. Masubuchi, J. P. Majewski, N. Torikai, N. L. Yamada, A. R. Siti Sarah, A. Takano, and Y. Matsushita, Macromolecules **44**, 9424 (2011).
[38]H. Arita, K. Mitamura, M. Kobayashi, N. L. Yamada, H. Jinnai, and A. Takahara, Polym. J. **45**, 117 (2013).
[39]T. Hayashi, K. Segawa, K. Sadakane, K. Fukao, and N. L. Yamada, J. Chem. Phys. **146**, 203305 (2017).
[40]V. F. Sears, Neutron News **3**, 26 (1992), SLD is evaluated from the scattering length of atoms given in this reference, together with the chemical composition of monomer and mass density of the polymer.
[41]N. L. Yamada, N. Torikai, K. Mitamura, H. Sagehashi, S. Sato, H. Seto, T. Sugita, S. Goko, M. Furusaka, T. Oda *et al.*, Eur. Phys. J. Plus **126**, 108 (2011).
[42]K. Mitamura, N. L. Yamada, H. Sagehashi, N. Torikai, H. Arita, M. Terada, M. Kobayashi, S. Sato, H. Seto, S. Goko *et al.*, Polym. J. **45**, 100 (2013).
[43]L. G. Parratt, Phys. Rev. **95**, 359 (1954).
[44]L. Névot and P. Croce, Rev. Phys. Appl. **15**, 761 (1980).
[45]A. Nelson, J. Appl. Crystallogr. **39**, 273 (2006).
[46]L. Onsager, Phys. Rev. **37**, 405 (1931).
[47]P. J. Flory, *Principles of Polymer Chemistry* (Cornell University Press, Ithaca, NY, 1953).
[48]M. Doi and S. F. Edwards, *The Theory of Polymer Dynamics*, International Series of Monographs on Physics Vol. 73, 1st ed. (Clarendon Press, Oxford, 1988), ISBN: 0-19-852033-6.
[49]G. Reiter, S. Huttenbach, M. Foster, and M. Stamm, Macromolecules **24**, 1179 (1991).
[50]R. J. Composto and E. J. Kramer, J. Mater. Sci. **26**, 2815 (1991).
[51]E. Jabbari and N. A. Peppas, Macromolecules **26**, 2175 (1993).
[52]E. Jabbari and N. A. Peppas, Polymer **36**, 575 (1995).
[53]K. Fukao, S. Uno, Y. Miyamoto, A. Hoshino, and H. Miyaji, Phys. Rev. E **64**, 051807 (2001).
[54]L. Hartmann, W. Gorbatschow, J. Hauwede, and F. Kremer, Eur. Phys. J. E **8**, 145 (2002).
[55]J. S. Sharp and J. A. Forrest, Phys. Rev. E **67**, 031805 (2003).
[56]A. Serghei, L. Hartmann, and F. Kremer, J. Non-Cryst. Solids **353**, 4330 (2007).
[57]D. S. Fryer, P. F. Nealey, and J. J. de Pablo, Macromolecules **33**, 6439 (2000).
[58]R. D. Priestley, D. Cangialosi, and S. Napolitano, J. Non-Cryst. Solids **407**, 288 (2015).
[59]X. Monnier and D. Cangialosi, Thermochim. Acta **677**, 60 (2019).